

See discussions, stats, and author profiles for this publication at: <https://www.researchgate.net/publication/341761209>

# Analysis of the First Core of the Indonesian Multipurpose Research Reactor RSG-GAS using the Monte Carlo Serpent Code and the ENDF/B-VIII.0 Nuclear Data Library

Article in Nuclear Engineering and Technology · May 2020

DOI: 10.1016/j.net.2020.05.027

CITATIONS

0

READS

39

2 authors:



**Donny Hartanto**

University of Sharjah

60 PUBLICATIONS 150 CITATIONS

[SEE PROFILE](#)



**Liem Peng Hong**

NAIS Co., Inc.

131 PUBLICATIONS 473 CITATIONS

[SEE PROFILE](#)

Some of the authors of this publication are also working on these related projects:



Physics Study of B&BR [View project](#)



Neutronics and Thermal-Hydraulics Models Validation via Uncertainty Propagation and Parameter Space Analysis [View project](#)



Contents lists available at ScienceDirect

## Nuclear Engineering and Technology

journal homepage: [www.elsevier.com/locate/net](http://www.elsevier.com/locate/net)

# Analysis of the first core of the Indonesian multipurpose research reactor RSG-GAS using the Serpent Monte Carlo code and the ENDF/B-VIII.0 nuclear data library

Donny Hartanto <sup>a, \*</sup>, Peng Hong Liem <sup>b, c</sup>

<sup>a</sup> Department of Mechanical and Nuclear Engineering, University of Sharjah, P.O. BOX 27272, Sharjah, United Arab Emirates

<sup>b</sup> Cooperative Major in Nuclear Energy, Graduate School of Engineering, Tokyo City University (TCU), 1-28-1, Tamazutsumi, Setagaya, Tokyo, Japan

<sup>c</sup> Scientific Computational Division, Nippon Advanced Information Service, (NAIS Co., Inc.), 416 Muramatsu, Tokaimura, Ibaraki, Japan

## ARTICLE INFO

## Article history:

Received 16 January 2020

Received in revised form

8 May 2020

Accepted 26 May 2020

Available online xxx

## Keywords:

RSG-GAS First core

SERPENT

ENDF/B-VIII.0

Critical benchmark

Sensitivity analysis

## ABSTRACT

This paper presents the neutronics benchmark analysis of the first core of the Indonesian multipurpose research reactor RSG-GAS (Reaktor Serba Guna G.A. Siwabessy) calculated by the Serpent Monte Carlo code and the newly released ENDF/B-VIII.0 nuclear data library. RSG-GAS is a 30 MWth pool-type material testing research reactor loaded with plate-type low-enriched uranium fuel using light water as a coolant and moderator and beryllium as a reflector. Two groups of critical benchmark problems are derived on the basis of the criticality and control rod calibration experiments of the first core of RSG-GAS. The calculated results, such as the neutron effective multiplication factor ( $k$ ) value and the control rod worth are compared with the experimental data. Moreover, additional calculated results, including the neutron spectra in the core, fission rate distribution, burnup calculation, sensitivity coefficients, and kinetics parameters of the first core will be compared with the previous nuclear data libraries (inter-library comparison) such as ENDF/B-VII.1 and JENDL-4.0. The C/E values of ENDF/B-VIII.0 tend to be slightly higher compared with other nuclear data libraries. Furthermore, the neutron reaction cross-sections of  $^{16}\text{O}$ ,  $^9\text{Be}$ ,  $^{235}\text{U}$ ,  $^{238}\text{U}$ , and  $S(\alpha, \beta)$  of  $^1\text{H}$  in  $\text{H}_2\text{O}$  from ENDF/B-VIII.0 have substantial updates; hence, the  $k$  sensitivities against these cross-section changes are relatively higher than other isotopes in RSG-GAS. Other important neutronics parameters such as kinetics parameters, control rod worth, and fission rate distribution are similar and consistent among the nuclear data libraries.

© 2020 Korean Nuclear Society, Published by Elsevier Korea LLC. This is an open access article under the CC BY-NC-ND license (<http://creativecommons.org/licenses/by-nc-nd/4.0/>).

## 1. Introduction

Recently, the Cross Section Evaluation Working Group, in collaboration with several international organizations has released a new ENDF/B-VIII.0 nuclear data library [1]. The new nuclear data cover neutron reaction libraries for 557 isotopes and thermal scattering libraries for 34 materials. The release is a significant improvement compared with its predecessor ENDF/B-VII.1, which has neutron reaction libraries for 423 isotopes and thermal scattering libraries for 21 materials [2]. Additionally, the new nuclear data adopts substantial updates for neutron reaction libraries such as  $^1\text{H}$ ,  $^9\text{Be}$ ,  $^{56}\text{Fe}$ ,  $^{235}\text{U}$ , and  $^{238}\text{U}$  [1] that affect the criticality calculation [3–5] including the first core of the Indonesian multipurpose

research reactor RSG-GAS.

The first core of RSG-GAS is a neutronics benchmark problem defined as a research reactor with 20% enriched  $\text{U}_3\text{O}_8$  fuel dispersed in the Al matrix using light water a moderator/coolant and beryllium reflectors [6]. The benchmark was derived from the reactor physics experiments during the first criticality of the reactor back in the mid of 1987. Only a few well-documented critical benchmark problems are available and open to the public based on a research reactor that uses 20% enriched uranium fuels. Therefore, the first core of the RSG-GAS benchmark problem is considered important, and it can be used to verify and validate the neutronics calculation tool and the nuclear data library to support the research reactor community as suggested by Komuro [7].

The benchmark problem consists of two different core configurations, one is the first criticality core that has nine fresh standard fuel elements and six control rod fuel elements, and another is the first working core of RSG-GAS that is made up of 12 fresh standard fuel

\* Corresponding author.

E-mail address: [dhartanto@sharjah.ac.ae](mailto:dhartanto@sharjah.ac.ae) (D. Hartanto).

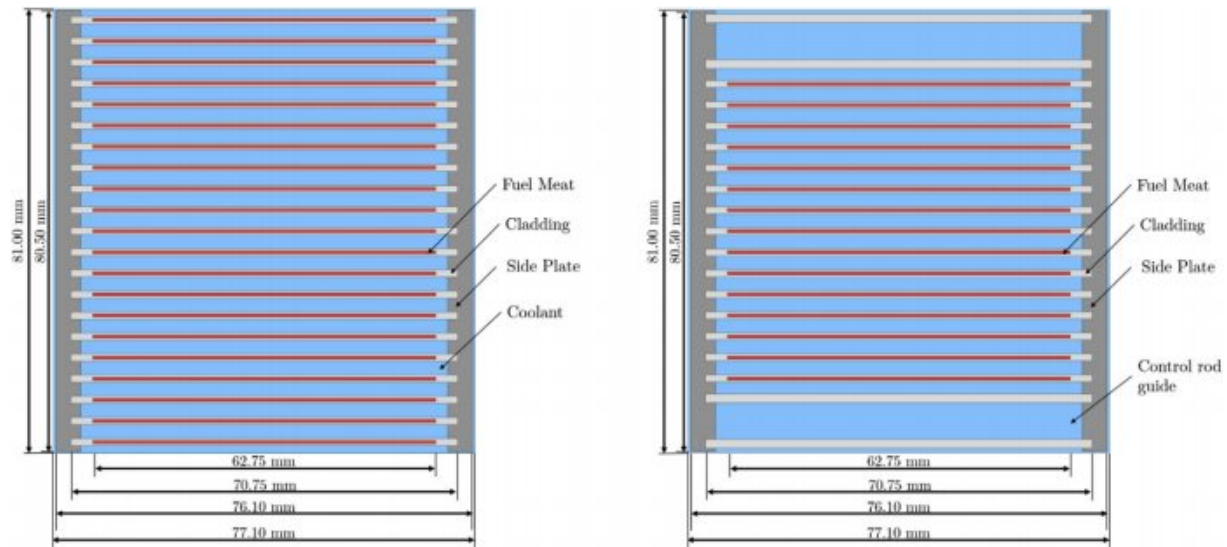


Fig. 1. Standard (left) and control (right) fuel element layout.

**Table 1**  
Major parameters of standard and control fuel elements [6].

Parameter	Value
Dimension (mm)	77.1 × 81 × 600
Fuel plate thickness (mm)	1.3
Coolant channel width (mm)	2.55
No. of plate per FE	21
No. of plate per CE	15
Fuel plate clad material	AlMg <sub>2</sub>
Fuel plate clad thickness (mm)	0.38
Fuel meat dimension (mm)	0.54 × 62.75 × 600
Fuel meat material	U <sub>3</sub> O <sub>8</sub> -Al
U-235 enrichment (wt%)	19.75
U density in meat (g/cc)	2.96
U-235 loading per FE (g)	250
U-235 loading per CE (g)	178.6
Absorber meat material	Ag-In-Cd
Absorber thickness (mm)	3.38
Absorber clad material	SS-321
Absorber clad thickness (mm)	0.85

elements and six control fuel elements. Liem [6] described the detail of the first core criticality experiment. Since the benchmark problem was established, extensive works such as criticality calculations using the Monte Carlo codes [6,8–12], criticality calculation using deterministic codes [13,14], and control rod worth calculation using the Monte Carlo and deterministic codes [15] have been done.

In this study, the new ENDF/B-VIII.0 is applied to these benchmark problems to investigate the impact of the newly released library on the RSG-GAS. The benchmark calculation work covers the effective neutron multiplication factor and control rod worth, which are compared against the experimental data. Furthermore, neutron spectra in the core, fission rate distributions, kinetics parameters, burnup calculation, and the sensitivity coefficients of the first core calculated using ENDF/B-VIII.0 are also compared with the ones with the previous version of nuclear data libraries such as ENDF/B-VII.1 [2] and JENDL-4.0 [16]. The calculations have been performed by using the 3-D continuous-energy Serpent Monte Carlo code [17]. The Monte Carlo method is recognized for its accuracy because it solves the neutron transport equation without any approximations, such as no simplification in the geometry and no discretization in the neutron energy. Conversely, the computing

time of the Monte Carlo method is expected to be longer. Nonetheless, the issue can be managed with the recent advancement in computing technology. The Serpent Monte Carlo code is chosen in this study because it is widely used and well verified and validated, including its application for the research reactor. Moreover, the computing speed of Serpent is expected to be faster because it adopts the unionized energy grid format and the Woodcock delta-tracking method [17].

The rest of this paper is organized as follows: Section 2 discusses the description of the RSG-GAS first core, Section 3 analyzes and deals with the results, and Section 4 presents the conclusions and recommendations for future works.

## 2. First core of RSG-GAS description

The RSG-GAS multipurpose research reactor is a pool-type material testing research reactor that is owned and operated by the Indonesian National Nuclear Energy Agency (BATAN). The location is in Serpong, West Java, and it can operate at a maximum power of 30 MWth for approximately 30 full power days and achieve the maximum discharge burnup up to 53.7%. The reactor uses low-enriched uranium (19.75% U-235) fuel using light water as a moderator and coolant, and beryllium reflectors. Initially, the fuel was U<sub>3</sub>O<sub>8</sub> dispersed in the Al matrix; however, it was converted to U<sub>3</sub>Si<sub>2</sub> fuel dispersed in the Al matrix. The typical working core was loaded with 40 standard and control fuel elements. Since it reached the first criticality in July 1987, RSG-GAS has been used for many applications, such as the production of medical and industrial radioisotopes, the irradiation of gemstones, and the testing of materials.

Fig. 1 and Table 1 show the standard and control fuel element configuration and parameters. As depicted, the standard fuel element (FE) consists of 21 fuel plates, while the control fuel element (CE) has 15 fuel plates to provide a space for the control rods. Each fuel plate contains 19.75% enriched U<sub>3</sub>O<sub>8</sub> meat dispersed in an aluminum matrix and surrounded by aluminum cladding on both sides of the fuel meat. The fuel plates are arranged and held by two Al side plates. Meanwhile, the control rod (CR) is a fork-type containing a silver-indium-cadmium absorber.

As mentioned above, two core configurations were documented during the experiment to achieve the first working core. Fig. 2

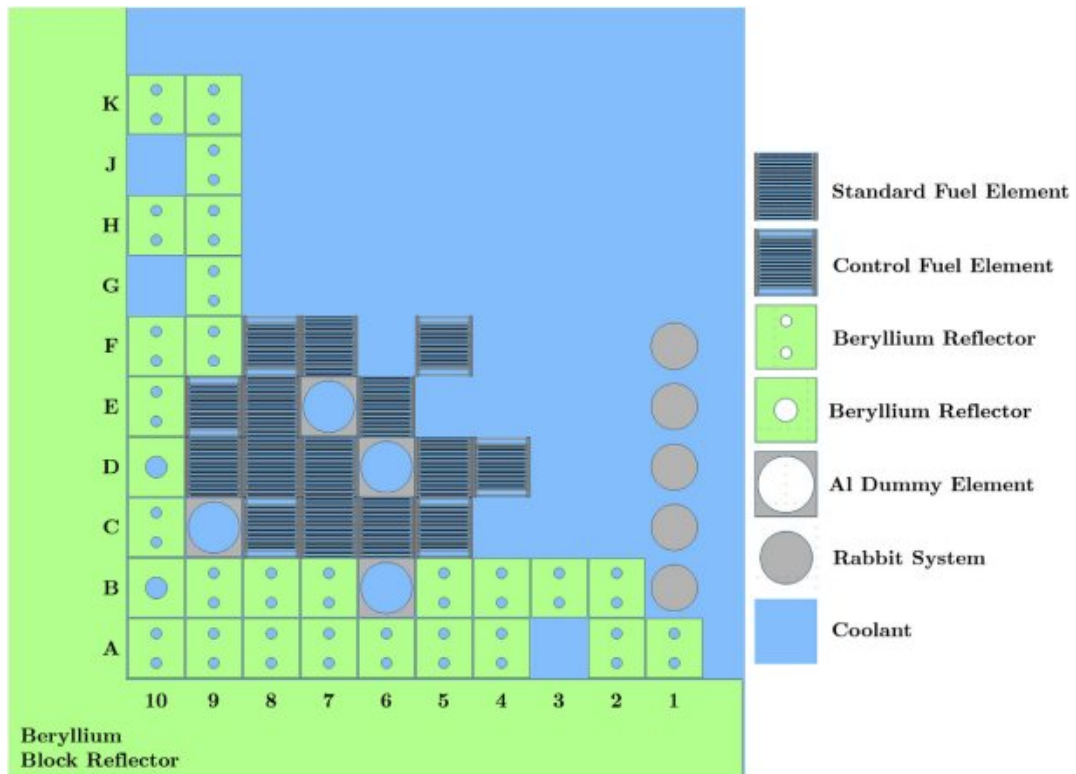


Fig. 2. First criticality core configuration of RSG-GAS.

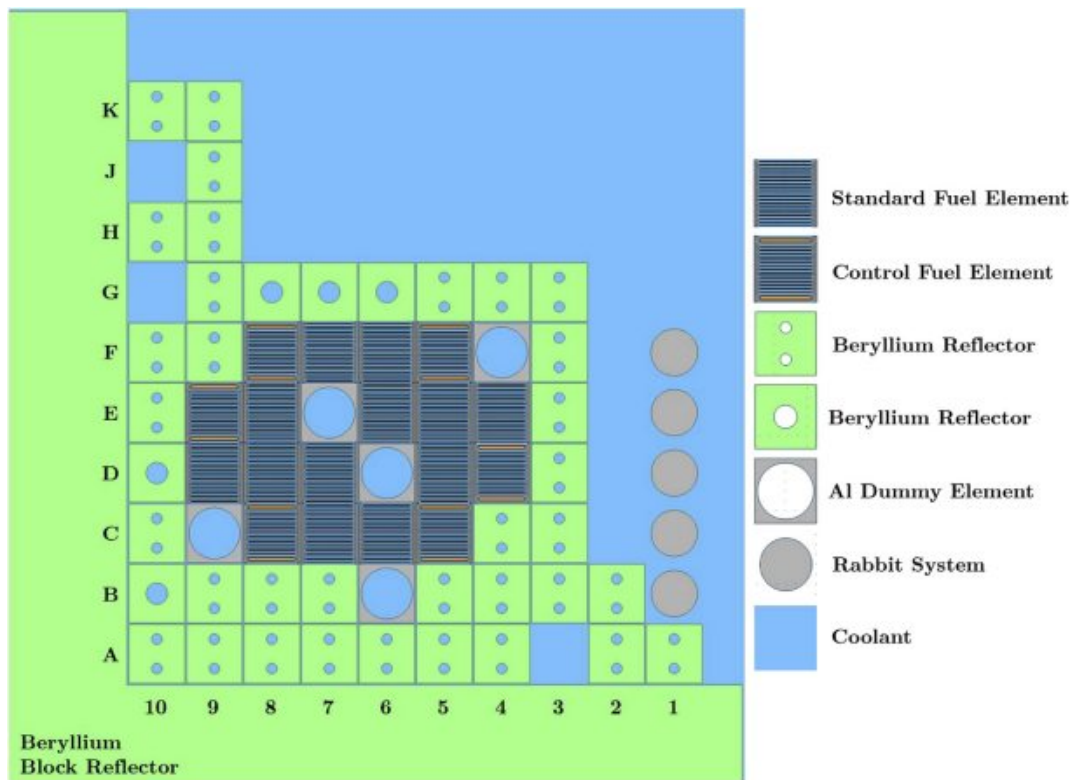


Fig. 3. First working core configuration of RSG-GAS.

**Table 2**

Calculation cases for the first core of RSG-GAS.

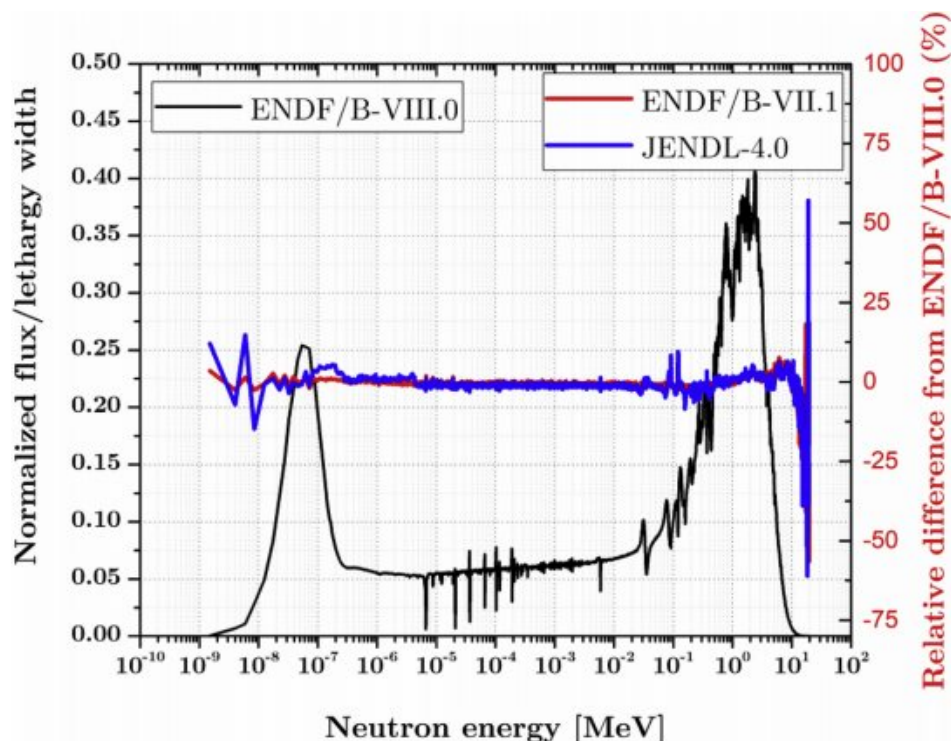
First group (First criticality and excess reactivity loading)	Remarks
First criticality (nine FEs, six CEs, RR inserted up to 475 mm)	Critical
Full core (12 FEs, six CEs, CRs all up)	Supercritical, $k = 1.09242$ [10]
Full core (12 FEs, six CEs, CRs all down)	Subcritical, CR worth = 17.18% [10]
Second group (Control rod calibrations, full core/12 FEs, six CEs)	Remarks
CR ID: JDA06 C-8 fully inserted, other rods inserted up to 290 mm	Critical
CR ID: JDA01 E-9 fully inserted, other rods inserted up to 284 mm	Critical
CR ID: JDA03 F-8 fully inserted, other rods inserted up to 293 mm	Critical
CR ID: JDA05 C-5 fully inserted, other rods inserted up to 288 mm	Critical
CR ID: JDA04 F-5 fully inserted, other rods inserted up to 290 mm	Critical
CR ID: JDA07 D-4 fully inserted, other rods inserted up to 282 mm	Critical

**Table 3**C/E of  $k$  for different nuclear data libraries.

First group	ENDF/B-VIII.0	ENDF/B-VII.1	JENDL-4.0
First criticality	1.0058	1.0051	1.0047
Full core (CRs all up)	1.0065	1.0064	1.0062
Full core (CRs all down)	N/A	N/A	N/A
Second group	ENDF/B-VIII.0	ENDF/B-VII.1	JENDL-4.0
CR ID: JDA06	1.0031	1.0030	1.0026
CR ID: JDA01	1.0031	1.0028	1.0025
CR ID: JDA03	1.0043	1.0041	1.0037
CR ID: JDA05	1.0043	1.0041	1.0038
CR ID: JDA04	1.0048	1.0045	1.0042
CR ID: JDA07	1.0045	1.0042	1.0038

depicts the smallest core arrangement that achieved the first criticality. Nine FEs are located at grids C-6, C-7, D-5, D-7, D-8, D-9, E-6, E-8, and F-7, while the six CEs are located at grids C-5, C-8, D-4, E-9, F-5, and F-8. The regulation rod (RR, positioned at grid C-8) was inserted slightly to make the core critical. By contrast, the first full working core configuration, illustrated in Fig. 3, consists of 12 FEs and six CEs. The locations of the six CEs are identical to the previous configuration. However, in addition to the nine FEs in the first criticality core, three more were added at grids E-4, E-5, and F-6. Moreover, the number of beryllium reflector surrounding the core was increased in the latter configuration to reduce the neutron leakage. This core configuration was made critical by inserting partial control rods into the core.

Table 2 summarizes the benchmark calculation cases of the first

**Fig. 4.** Neutron spectra for different nuclear data libraries.



**Table 4**  
Effect of specific isotope neutron reaction library from ENDF/B-VIII.0 on  $k$  of other nuclear data libraries.

Isotopes from ENDF/B-VIII.0	ENDF/B-VII.1	JENDL-4.0
$^{27}\text{Al}$ in fuel	$-7.00 \pm 4.67$	$-2.00 \pm 4.67$
$^{27}\text{Al}$ in structural	$-4.00 \pm 4.67$	$-29.00 \pm 4.60$
$^9\text{Be}$	$-28.00 \pm 4.67$	$-165.00 \pm 4.60$
$^1\text{H}$	$-56.00 \pm 4.67$	$-51.00 \pm 4.60$
$^{16}\text{O}$ in fuel	$-12.00 \pm 4.60$	$0.00 \pm 4.60$
$^{16}\text{O}$ in coolant	$-93.00 \pm 4.67$	$-148.00 \pm 4.67$
$^{235}\text{U}$	$59.00 \pm 4.60$	$72.00 \pm 4.60$
$^{238}\text{U}$	$28.00 \pm 4.60$	$47.00 \pm 4.60$
$S(\alpha,\beta)$ of $^1\text{H}$ in $\text{H}_2\text{O}$	$-29.00 \pm 4.67$	$180.00 \pm 4.60$
$S(\alpha,\beta)$ of $^9\text{Be}$	$-8.00 \pm 4.67$	$4.00 \pm 4.67$

core of RSG-GAS performed in this work and categorizes them into the first and second groups. The first group has three cases, but only the first criticality case was measured directly during the criticality approach experiment. The other two cases were derived on the basis of the incorporation of the experimental result and additional analytical calculation [8,10]. Meanwhile, the second group has six critical cases, and they were evaluated directly from the control rod calibration experiment. Each case in the second group is identified by its corresponding control rod identification number such as JDA01 for the control rod at grid E-9.

**3. Analysis results and discussion**

Before dealing with the results, the 3-D calculation model and condition are discussed briefly, and the geometry of the active region of the first core RSG-GAS in this work is modeled explicitly. However, homogenized mixture models by conserving the volume of each region are used for the top and end-fitting regions of the elements, core grid, and bottom supports. This approach is expected to have a negligible impact on the criticality calculation because they are located outside of the active core region. All components in the core have a temperature of 300 K. The Serpent

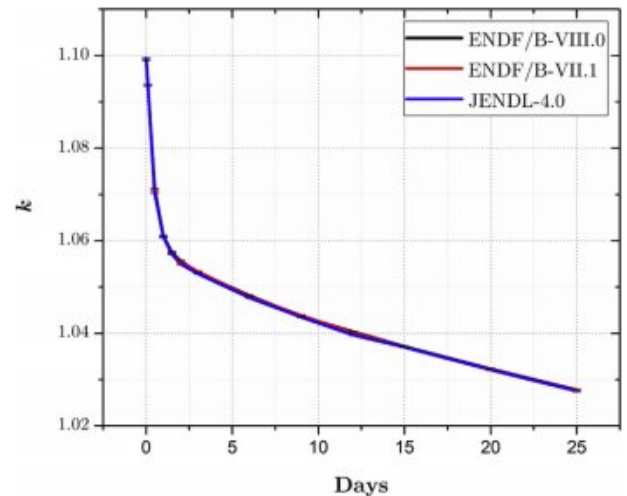


**Fig. 6.**  $k$  as a function of burnup for different nuclear data libraries.

Monte Carlo code has been used with 400,000 neutron histories per cycle, and the total number of cycles is 2200 with 200 inactive cycles. Using this calculation conditions, the standard deviation of  $k$  is less than 4 pcm. Moreover, the thermal scattering libraries  $S(\alpha,\beta)$  for hydrogen in the light water and beryllium as metal are included in the calculation.

Table 3 compares the ratio of the  $k$  values of Serpent to the experimental values for different nuclear data libraries and for core configurations. Overall, the calculation results are very close to the experimental results taking into account the uncertainties due to nuclear data is about 0.006 [11], and the new ENDF/B-VIII.0 provides slightly higher  $k$  values than other libraries. The highest overestimation was observed for the full core configuration without any insertion of control rods (1st group, 2nd case), which is nearly 0.646%. It was expected as the reference  $k$  value was not purely experimental data. During the experiment, the excess reactivity

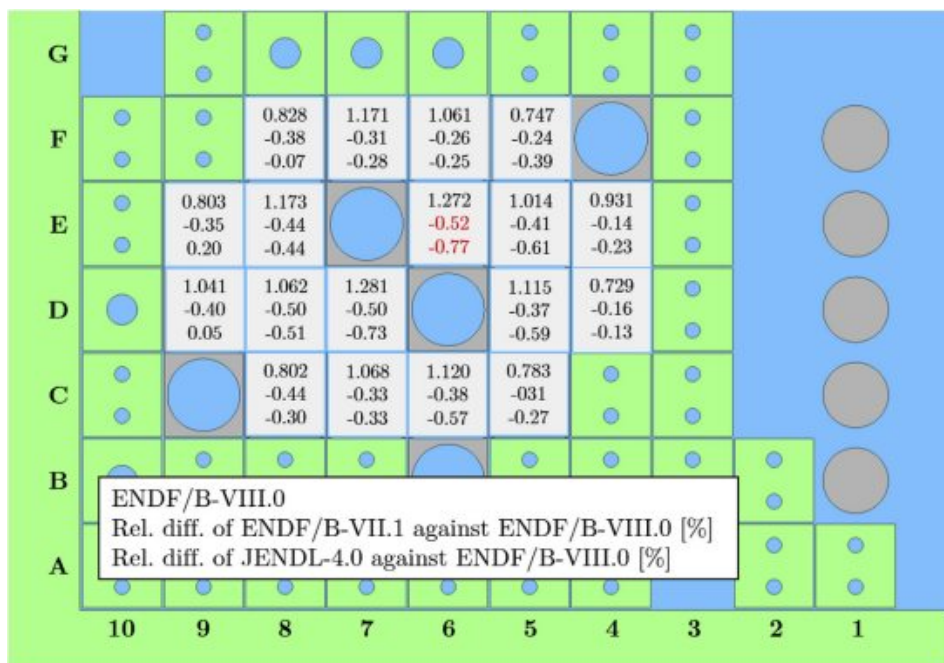


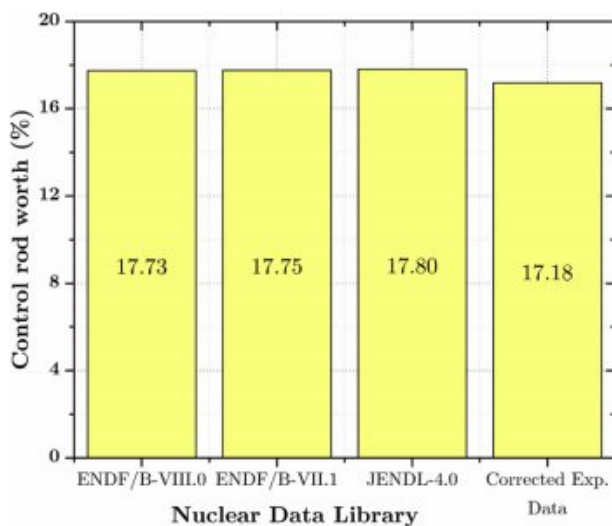
**Fig. 5.** Relative radial fission power distribution for different nuclear data libraries.

**Table 5**  
Positive sensitivities of  $k$ .

Isotope	Reaction	ENDF/B-VIII.0	Ratio of ENDF/B-VII.1 to ENDF/B-VIII.0	Ratio of JENDL-4.0 to ENDF/B-VIII.0
$^{235}\text{U}$	$\bar{\nu}$ prompt	9.878E-01	1.00	1.00
$^{235}\text{U}$	(n,f)	3.503E-01	1.00	1.00
$^1\text{H}$	(n,el)	2.922E-01	1.01	1.01
$^9\text{Be}$	(n,el)	5.967E-02	1.02	1.01
$^{16}\text{O}$	(n,el)	4.275E-02	1.02	1.00
$^1\text{H}$	S( $\alpha,\beta$ )	2.807E-02	0.92	1.07
$^{27}\text{Al}$	(n,el)	2.767E-02	1.00	1.05
$^9\text{Be}$	(n,xn)	1.100E-02	1.03	1.05
$^{27}\text{Al}$	(n,inl)	1.082E-02	1.02	0.93
$^9\text{Be}$	S( $\alpha,\beta$ )	7.394E-03	0.91	0.64
$^{235}\text{U}$	$\bar{\nu}$ delayed	7.281E-03	1.01	1.01
$^{238}\text{U}$	$\bar{\nu}$ prompt	4.806E-03	1.01	1.03
$^{238}\text{U}$	(n,el)	4.675E-03	0.97	1.03
$^{238}\text{U}$	(n,f)	3.373E-03	1.01	1.01
$^{238}\text{U}$	(n,inl)	2.032E-03	1.04	1.13
$^{56}\text{Fe}$	(n,el)	1.752E-03	0.98	1.04

**Table 6**  
Negative sensitivities of  $k$ .

Isotope	Reaction	ENDF/B-VIII.0	Ratio of ENDF/B-VII.1 to ENDF/B-VIII.0	Ratio of JENDL-4.0 to ENDF/B-VIII.0
$^1\text{H}$	(n,g)	-1.679E-01	1.00	1.01
$^{235}\text{U}$	(n,g)	-1.237E-01	0.99	0.99
$^{27}\text{Al}$	(n,g)	-5.061E-02	1.01	0.99
$^{238}\text{U}$	(n,g)	-3.758E-02	1.01	1.02
$^9\text{Be}$	(n,g)	-8.391E-03	1.01	0.93
$^{55}\text{Mn}$	(n,g)	-4.346E-03	1.01	1.02
$^{109}\text{Ag}$	(n,g)	-3.388E-03	1.01	1.02
$^{115}\text{In}$	(n,g)	-2.450E-03	0.97	0.98
$^{107}\text{Ag}$	(n,g)	-1.777E-03	1.02	1.04
$^{16}\text{O}$	(n,g)	-1.759E-03	0.76	0.75
$^{113}\text{Cd}$	(n,g)	-1.351E-03	1.03	0.96
$^{56}\text{Fe}$	(n,g)	-1.217E-03	1.02	1.01

**Fig. 7.** Control rod worth for different nuclear data libraries.

was evaluated by the summation of the individually measured control rod reactivity, and the interference effect of the control rod was neglected. Moreover, the excess reactivity was initially in a unit of \$, and it was converted later using the  $\beta_{eff}$  (total effective delayed neutron fraction) value calculated by the Monte Carlo method as the measured  $\beta_{eff}$  value was unavailable [10].

For the achievement of prime insight into the new ENDF/B-VIII.0 nuclear data library, the neutron spectra in the fuel meat are

compared in Fig. 4, the effect of the neutron cross-section of the specific isotope from ENDF/B-VIII.0 is investigated and presented in Table 4, and the radial power distribution is plotted in Fig. 5. The calculation was performed for the full core configuration without any control rods (1st group, 2nd case). Fig. 4 depicts that a sharp increase arises in the relative difference of the spectra at the high neutron energy region, which is regarded as likely as the neutron flux at that energy is fairly low and thus the uncertainty of flux for that energy region calculated by Serpent is high. However, the neutron spectrum by JENDL-4.0 has a higher relative difference to ENDF/B-VIII.0 compared with ENDF/B-VII.1.

Table 4 shows the effect of the neutron cross-section library of several main isotopes in RSG-GAS from ENDF/B-VIII.0 on the  $k$  value of other nuclear data libraries. For ENDF/B-VII.1, the maximum decrease of  $k$  is given by  $^{16}\text{O}$  (in coolant) roughly 93 pcm, followed by  $^1\text{H}$  (in coolant) approximately 56 pcm, S( $\alpha,\beta$ ) of H in  $\text{H}_2\text{O}$  nearly 29 pcm, and  $^9\text{Be}$  roughly 28 pcm from ENDF/B-VIII.0, and  $k$  increases approximately 59 pcm when  $^{235}\text{U}$  from ENDF/B-VIII.0 is used. For JENDL-4.0, replacing  $^9\text{Be}$  and  $^{16}\text{O}$  (in coolant) with ENDF/B-VIII.0 decreases  $k$  by roughly 165 pcm and 148 pcm, respectively, whereas replacing S( $\alpha,\beta$ ) of H in  $\text{H}_2\text{O}$ ,  $^{235}\text{U}$ , and  $^{238}\text{U}$  with ENDF/B-VIII.0 increases  $k$  by nearly 180 pcm, 72 pcm, and 47 pcm, respectively. It is worth mentioning that  $^1\text{H}$ ,  $^{16}\text{O}$ ,  $^{235}\text{U}$ , and  $^{238}\text{U}$  are the isotopes that have major updates in ENDF/B-VIII.0 from CIELO (Collaborative International Evaluated Library Organization) evaluations [18]. Isotope Be-9 and S( $\alpha,\beta$ ) for H in  $\text{H}_2\text{O}$  were also updated in ENDF/B-VIII.0 [1].

The relative fission rate distribution is calculated by scoring the fission reaction rate using the reaction multiplier in Serpent. The result illustrated in Fig. 5 shows the peak-to-average radial fission

**Table 7**  
Kinetics parameters for different nuclear data libraries.

First group	Kinetics Parameters	ENDF/B-VIII.0	ENDF/B-VII.1	JENDL-4.0	Abs. RMSE
First criticality	$\beta_{\text{eff}}$ (pcm)	747.16 ± 1.6	747.44 ± 1.6	749.30 ± 1.6	0.95
	$\Lambda$ ( $\mu\text{s}$ )	84.06 ± 0.04	84.95 ± 0.04	86.81 ± 0.04	1.14
	$\alpha$ (1/s)	-88.84 ± 0.20	-87.94 ± 0.19	-86.27 ± 0.19	1.07
Full core (CRs all up)	$\beta_{\text{eff}}$ (pcm)	730.01 ± 1.4	730.08 ± 1.4	730.30 ± 1.5	0.12
	$\Lambda$ ( $\mu\text{s}$ )	73.91 ± 0.03	74.69 ± 0.03	76.20 ± 0.03	0.95
	$\alpha$ (1/s)	-98.82 ± 0.20	-97.83 ± 0.19	-95.61 ± 0.19	1.34
Full core (CRs all down)	$\beta_{\text{eff}}$ (pcm)	742.94 ± 1.7	743.42 ± 1.7	744.74 ± 1.7	0.76
	$\Lambda$ ( $\mu\text{s}$ )	67.70 ± 0.03	68.32 ± 0.03	69.38 ± 0.03	0.70
	$\alpha$ (1/s)	-109.73 ± 0.26	-108.79 ± 0.26	-107.31 ± 0.25	0.99

power distribution in each fuel elements. It is shown that there is a good agreement among the three libraries with a relative difference of less than 0.8%.

A hypothetical depletion calculation was also performed for the same core configuration with all control rods withdrawn. The thermal power was set to 10 MWth in the calculation to accommodate a small core size, and it was depleted up to 25 days. The Chebyshev Rational Approximation Method was selected as the depletion algorithm, while linear extrapolation and linear interpolation are adopted for the predictor and corrector methods, respectively, as recommended [19]. For each library, its corresponding version of radioactive decay data and neutron fission yield data was used. Fig. 6 depicts that the  $k$  values as the function of burnup among the three libraries are consistent, and the fraction losses of  $^{235}\text{U}$  after 25 days for ENDF/B-VIII.0, ENDF/B-VII.1, and JENDL-4.0 are 7.617%, 7.605%, and 7.602%, respectively, which shows excellent agreement among the nuclear data libraries. However, the impact of the updated decay data library can be considered small in this hypothetical burnup calculation as the power used is small and the total burn days are 25 days.

The  $k$  sensitivity analysis was also performed for the 1st case of the 2nd group (CR ID: JDA06) where the control rod was calibrated; thus, the sensitivity of the isotopes and reactions in the control absorber can be analyzed. The  $k$  sensitivity is defined as the ratio between the relative change in  $k$  to the relative change in parameters such as cross section and  $\bar{\nu}$  (average number of neutrons per fission). In Serpent, the sensitivity is calculated by the collision history method [20]. The results are presented in Tables 5 and 6 for positive and negative sensitivities to  $k$ , respectively. Only the sensitivities that have an absolute value larger than 0.1% are shown and the ratio of calculated sensitivity using ENDF/B-VII.1 or JENDL-4.0 to ENDF/B-VIII.0 that has an absolute difference larger than 5% are highlighted in grey. Table 5 exhibits that the elastic scattering is the dominant reaction contributing to the positive sensitivities, followed by others such as  $\bar{\nu}$ , fission,  $S(\alpha, \beta)$ , inelastic scattering, and neutron production ( $n, xn$ ). The top five contributors in Table 5 are  $\bar{\nu}$  prompt and ( $n, f$ ) of  $^{235}\text{U}$ , ( $n, el$ ) of  $^1\text{H}$ ,  $^9\text{Be}$ , and  $^{16}\text{O}$ , and  $S(\alpha, \beta)$  of  $^1\text{H}$  in  $\text{H}_2\text{O}$ . Meanwhile, in Table 6, the dominant reaction of the negative sensitivities is neutron capture, and the top 5 contributors are  $^1\text{H}$ ,  $^{235}\text{U}$ ,  $^{27}\text{Al}$ ,  $^{238}\text{U}$ , and  $^9\text{Be}$ . These results are also consistent with the previous sensitivities produced by Whisper-1.1 and ENDF/B-VII.1 [11]. With regard to the inter-library comparison, JENDL-4.0 produces significant differences compared with ENDF/B-VIII.0, especially for  $S(\alpha, \beta)$  of  $^9\text{Be}$ , ( $n, g$ ) of  $^{16}\text{O}$ , ( $n, inl$ ) of  $^{238}\text{U}$ ,  $S(\alpha, \beta)$  of  $^1\text{H}$  in  $\text{H}_2\text{O}$ , ( $n, inl$ ) of  $^{27}\text{Al}$ , and ( $n, g$ ) of  $^9\text{Be}$ , while ENDF/B-VII.1 provides significant differences for ( $n, g$ ) of  $^{16}\text{O}$  and  $S(\alpha, \beta)$  of  $^9\text{Be}$  and  $^1\text{H}$  in  $\text{H}_2\text{O}$ . These results are clearly reflected in Table 4 when the specific isotope neutron reaction library from ENDF/B-VIII.0 is used.

The total control rod worth is compared in Fig. 7, and it is defined as the reactivity difference when all control rods are withdrawn and inserted. During the experiment, the worth of each

control rod was measured by the shim rod bank compensation method, and the arithmetic summation of each control rod worth was done to obtain the total control rod worth, without considering the rod shadowing effect. Accordingly, the difference is noticed between the experimental and calculated results. However, the total control rod worth of the three nuclear data libraries agrees very well with an absolute root mean square error (RMSE) of 0.03.

The calculated kinetics parameters,  $\beta_{\text{eff}}$  (total effective delayed neutron fraction)  $\Lambda$  (prompt neutron generation lifetime), and  $\alpha$  (Rossi-alpha value) are summarized in Table 7 for the core configurations in the 1st group. The kinetics parameters were calculated using the adjoint method available in Serpent, specifically by the iterated fission probability method. Generally, the value of the kinetics parameters for each core is consistent among the three nuclear data libraries with the maximum absolute RMSEs of 0.95, 1.14, 1.34 for  $\beta_{\text{eff}}$ ,  $\Lambda$ , and  $\alpha$  respectively.

#### 4. Conclusions

The newly released ENDF/B-VIII.0 nuclear data library has been adopted to characterize several important neutronics parameters of the first core of the Indonesian multipurpose research reactor RSG-GAS benchmark problem. The Serpent Monte Carlo code has been used as the calculation tool. Moreover, the C/E of the  $k$  values by ENDF/B-VIII.0 tends to be slightly higher than other nuclear data libraries, and the maximum value is approximately 1.00646 for the full working core configuration when all the control rods are withdrawn. The  $^{16}\text{O}$  neutron cross from ENDF/B-VIII.0 provides the largest reduction to the  $k$  value of ENDF/B-VII.1 and using  $^9\text{Be}$  and  $^{16}\text{O}$  neutron cross sections from ENDF/B-VIII.0 contributes largely to the decrease of the  $k$  value of JENDL-4.0. On the one hand, replacing  $S(\alpha, \beta)$  of  $^1\text{H}$  in  $\text{H}_2\text{O}$ ,  $^{235}\text{U}$  and  $^{238}\text{U}$  neutron cross sections from ENDF/B-VIII.0 cause the increase of the  $k$  value of JENDL-4.0. These isotopes also produce relatively high sensitivity coefficients of  $k$ . On the other hand, the kinetics parameters, control rod worth, fission rate distribution, and average burnup in %loss of  $^{235}\text{U}$  are consistent among the nuclear data libraries. In the future, the uncertainty analysis of  $k$  using ENDF/B-VIII.0 is planned to be conducted.

#### Declaration of competing interest

The authors declare that they have no known competing financial interests or personal relationships that could have appeared to influence the work reported in this paper.

#### Appendix A. Supplementary data

Supplementary data to this article can be found online at <https://doi.org/10.1016/j.net.2020.05.027>.



## References

- [1] D.A. Brown, et al., ENDF/B-VIII.0: the 8<sup>th</sup> major release of the nuclear reaction data library with CIELO-project cross sections, new standards and thermal scattering data, Nucl. Data Sheets 148 (2018) 1–42.
- [2] M.B. Chadwick, et al., ENDF/B-VII.1 nuclear data for science and technology: cross sections, covariances, fission product yields and decay data, Nucl. Data Sheets 112 (12) (2011) 2887–2996.
- [3] O. Kabach, et al., Processing and benchmarking of evaluated nuclear data file/B-VIII.0β4 cross-section library by analysis of a series of critical experimental benchmark using the Monte Carlo code MCNP(X) and NJOY2016, Nucl. Eng. Technol. 49 (8) (2017) 1610–1616.
- [4] O. Kabach, et al., Processing of JEFF-3.3 and ENDF/B-VIII.0 and testing with critical benchmark experiments and TRIGA mark II research reactor using MCNPX, Appl. Radiat. Isot. 150 (2019) 146–156.
- [5] H.J. Park, et al., Comparison of ENDF/B-VIII.0 and ENDF/B-VII.1 in criticality, depletion benchmark, and uncertainty analyses by McCARD, Ann. Nucl. Energy 131 (2019) 443–459.
- [6] P.H. Liem, Monte Carlo calculations on the first criticality of the multipurpose reactor G.A. Siwabessy, At. Indones. 24 (2) (1998) 51–57.
- [7] Y. Komuro, A proposal to asian countries with operating research reactors for making nuclear criticality safety benchmark evaluations, J. Nucl. Sci. Technol. 37 (6) (2000) 548–554.
- [8] P.H. Liem, T.M. Sembiring, Benchmarking the new JENDL-4.0 library on criticality experiments of research reactor with oxide LEU (20w/o) fuel, light water moderator and beryllium reflectors, Ann. Nucl. Energy 44 (2012) 58–64.
- [9] T.M. Sembiring, P.H. Liem, Accuracy of the ENDF/B-VII.0 nuclear data library on the first criticality experiments of the Indonesian multipurpose reactor RSG GAS, in: Proceedings of the 2013 International Conference on Nuclear Data for Science and Technology (ND2013), 2013. New York, USA, March 4–8.
- [10] P.H. Liem, et al., Kinetics parameters evaluation on the first core of the RSG GAS (MPR-30) using continuous energy Monte Carlo method, Prog. Nucl. Energy 109 (2018) 196–203.
- [11] P.H. Liem, et al., Sensitivity and uncertainty analysis on the first core criticality of the RSG GAS multipurpose research reactor, Prog. Nucl. Energy 114 (2019) 46–60.
- [12] D. Hartanto, et al., Benchmarking the new ENDF/B-VIII.0 nuclear data library for the first core of Indonesian multipurpose research reactor (RSG-GAS), in: Proceedings of 2019 International Conference on Nuclear Data for Science and Technology (ND2019), Beijing, China, 2019. May 19–24.
- [13] P.H. Liem, “Validation of BATAN’s standard 3-D diffusion code, BATAN-3DIFF, on the first core of RSG GAS, At. Indones. 25 (1) (1999) 47–64.
- [14] S. Pinem, J. Susilo, Validation of the SRAC code on the first core of RSG-GAS reactor, in: Proceedings of the FNCA 2006 Workshop of the Utilization of Research Reactors, 2006. Manila, Philippines, August 28–September 1.
- [15] T. Surbakti, et al., Calculation of control rods reactivity worth of RSG-GAS first core using deterministic and Monte Carlo methods, At. Indones. 45 (2) (2019) 69–79.
- [16] K. Shibata, et al., JENDL-4.0: a new library for nuclear science and engineering, J. Nucl. Sci. Technol. 48 (1) (2011) 1–30.
- [17] J. Leppänen, et al., The Serpent Monte Carlo code: status, development and applications in 2013, Ann. Nucl. Energy 82 (2015) 142–150.
- [18] M.B. Chadwick, et al., The CIELO collaboration: neutron reactions on <sup>1</sup>H, <sup>16</sup>O, <sup>56</sup>Fe, <sup>235,238</sup>U, and <sup>239</sup>Pu, Nucl. Data Sheets 118 (2014) 1–25.
- [19] A.E. Isotalo, P.A. Aarnio, Higher order methods for burnup calculations with bateman solutions, Ann. Nucl. Energy 38 (2011) 1987–1995.
- [20] M. Aufiero, et al., A collision history-based approach to sensitivity/perturbation calculations in the continuous energy Monte Carlo code serpent, Ann. Nucl. Energy 85 (2015) 245–258.